ELSEVIER

Dynamics of Atmospheres and Oceans 32 (2000) 209–237

dynamics of atmospheres and oceans

www.elsevier.com/locate/dynatmoce

Numerical simulations of the North Atlantic subtropical gyre: sensitivity to boundary conditions

Alfonso M. Paiva [1], Eric P. Chassignet [*], Arthur J. Mariano

Division of Meteorology and Physical Oceanography, Rosenstiel School of Marine and Atmospheric Science, University of Miami, 4600 Rickenbacker Causeway, Miami, FL 33149, USA

Received 23 October 1998; received in revised form 15 June 1999; accepted 25 July 1999

Abstract

A series of simulations have been carried out with the Miami Isopycnic Coordinate Ocean Model (MICOM) in the context of the Data Assimilation and Modeling Evaluation Experiment-North Atlantic Basin (DAMÉE-NAB), in order to explore the model's ability to reproduce the wind- and thermohaline-driven circulations in the North Atlantic subtropical gyre. This paper addresses the constraints imposed on the simulations by the domain size and by the position of the ocean lateral boundaries. Comparisons between simulations performed in a large CME-like domain (28°S to 65°N) and in a smaller DAMÉE-NAB domain (6°N to 50°N) are discussed in detail. In the large configuration, the flow into the subtropics is related to the model circulation in the subpolar and equatorial regions, while in the smaller configuration, that flow depends solely on the interaction between the circulation in the subtropics and the restoring forcing at the boundaries. Despite the fact that the boundaries in the small domain are located adjacent to the region of interest, and that these boundaries intersect strong meridional surface flows in the western basin (in contrast to the situation in the large domain), the restoring force is able to generate appropriate inflow and outflow conditions without significantly disrupting the circulation in the subtropical gyre.

The impact of grid spacing is also assessed by doubling the horizontal resolution. This increase in resolution implies an increase in the number of grid points inside the buffer zones, which modifies the vertical mass transfer within the boundaries and consequently the efficiency of the buffer zones. This is shown to be particularly important in the sponge layer located in the Gulf of Cádiz to simulate the outflow of salty Mediterranean waters into the North Atlantic, which under certain circumstances, can significantly modify the interior water mass properties. Furthermore,

[*] Corresponding author.

E-mail address: echassignet@rsmas.miami.edu (E.P. Chassignet).

[1] Now at COPPE/PEnO, Universidade Federal do Rio de Janeiro, Cidade Universitaria, CT, sala 203, Rio de Janeiro, RJ, 21945-970, Brazil.

PII: S0377-0265(00)00048-8

changes in the flow conditions in the Gulf of Cádiz, associated with this increase in resolution, also have an important impact upon the model's ability to simulate the Azores Current.

Keywords: North Atlantic; Sensitivity; Boundary conditions

1. Introduction

Ocean general circulation models (OGCMs) are widely used in physical oceanography in order to increase our understanding of the oceans, by providing realistic representations of the large scale circulation and tracer distribution. Model configurations vary depending upon the problem, from simple box models to state-of-the-art global simulations [see McWilliams (1998) for a review]. While one may envision a fully eddy-resolving global coupled ocean–atmosphere GCM as the ultimate achievement in numerical modeling, limitations on our ability to understand the complex phenomena arising from the full physics, coupled with the availability of a finite amount of computer time, make simpler model configurations attractive. To that end, ocean models are often configured with limited area domains. This approach, however, introduces complicating factors in the interpretation of model results due to the implementation of lateral boundary conditions at the edges of the domain.

Truly open boundary conditions, in which fluxes are specified at the boundaries, are not widely used in basin-wide simulations mainly due to the lack of information about those fluxes. It can also be argued that open boundary conditions reduce the number of degrees of freedom of the model solutions, which are forced to agree with a pre-interpretation of the circulation at the boundaries. A more common approach for the implementation of oceanic boundary conditions, mostly because of its simplicity, has been to treat open boundaries as closed, but outfitted with buffer zones (sponge layers) in which temperature and salinity are linearly relaxed (restored) toward their seasonally varying climatological values. The main reason for use of the restoring forcing is to induce the thermohaline circulation by: (a) approximately recovering the climatological vertical shear of the currents; and (b) generating water property transformations which in reality would be accomplished in latitudes outside the model domain. The adequacy of this approach is strongly dependent upon poorly known oceanic climatologies and upon the circulation generated by the model within the buffer zones (Klinck, 1995). In particular, there is no prescription of the barotropic flow, which is free to evolve with the solution (away from the solid walls). In general, there can be no guarantee that this type of boundary condition will produce the appropriate mass, heat, and salt fluxes in the interior domain. Several papers have addressed the limitations of the buffer zone approach (Holland and Bryan, 1994; Döscher et al., 1994; Beckmann et al., 1994; Klinck, 1995; Smith et al., 2000) in the context of the North Atlantic Community Modeling Experiment (CME), in which the northern and southern boundaries are placed at 65°N and 15°S, respectively. The choice of these latitudes places the northern boundary downstream of the Denmark Straits overflow and the southern boundary away from the energetic equatorial region.

In this paper, the impact of the lateral boundary positions on the model circulation in the North Atlantic subtropics is investigated in detail within the framework of the Data Assimilation and Modeling Evaluation Experiment-North Atlantic Basin (DAMÉE-NAB) as a function of domain size and grid resolution. The model configuration for DAMÉE-NAB was chosen to cover the subtropical gyre from 6°N to 50°N. In contrast to the CME configuration, the northern boundary intersects a strong meridional flow (the North Atlantic Current) while the southern boundary is located in a region of large seasonal variation both in meridional heat transport and in the direction of the surface flow (the latter variation being associated with the seasonal behavior of the North Equatorial Counter Current). The consequences of placing buffer zones at these latitudes are evaluated, and the model results are compared to observations and to the results of simulations in CME-like configurations.

The impact of grid resolution is assessed by refining the model horizontal grid from 1° to 0.5°. This implies an increase in the number of grid points inside the buffer zones (for a given width of the buffer zones), through which diabatic water mass conversions take place. Such an increase modifies the vertical mass transfer within the boundaries and consequently the efficiency of the buffer zones (Beckmann et al., 1994; Smith et al., 2000). This is particularly important for the sponge layer located in the Gulf of Cádiz to simulate the outflow of salty Mediterranean waters into the North Atlantic, which, under certain circumstances, can significantly modify the interior water mass properties. Furthermore, changes in the flow conditions in the Gulf of Cádiz, associated with this increase in resolution, also have an important impact upon the model's ability to simulate the Azores Current.

Varying both the grid resolution and the restoring forcing at the boundaries also leads to diverging representations of the western boundary current, especially its separation from the coast. The issue of resolution also applies to the spatial resolution of the surface thermodynamic forcing derived from atmospheric climatologies. Ship-based climatologies, which are often employed in large scale modeling, typically represent phenomena with length scales larger than ~ 1000 km, and cannot reproduce strong atmospheric or oceanic frontal systems such as the thermal front along the axis of the Gulf Stream. It has been argued by Ezer and Mellor (1992) and by Chassignet et al. (1995) that surface heat fluxes may play an important role in the separation and path of the Gulf Stream while contributing to the preservation of the density structure of slope waters. The impact on western boundary current behavior of a heat flux derived from a recent sea surface temperature (SST) climatology based on AVHRR satellite observations, which differs from ship-based climatologies by a sharper definition of the SST front associated with the Gulf Stream, is therefore also investigated and discussed.

This paper is organized as follows: the various model configurations that differ in domain size, boundary conditions, and/or grid resolution are presented in Section 2. In Section 3, the model spin up and the water mass transformations that occur in the subtropical gyre in the DAMÉE-NAB configuration are compared to those that occur in an extended CME-like configuration. The impact of the model configuration is then further investigated in Section 4 for the meridional overturning streamfunction and associated heat transport, and in Section 5, for the surface circulation. The results are summarized and discussed in Section 6.

2. Model configuration

The simulations were carried out with the Miami Isopycnic Coordinate Ocean Model (MICOM). The model is well documented in the literature, and the reader is referred to Bleck et al. (1992) and Bleck and Chassignet (1994) for a review. The most significant aspect of the MICOM architecture is the vertical discretization in layers of constant density. The fundamental reason for modeling ocean flow in density coordinates is that this system suppresses the diapycnal component of numerically caused dispersion of material and thermodynamic properties (temperature, salinity, ...). This characteristic allows isopycnic models to prevent the spurious warming of deep water masses, as has been shown to occur in models framed in Cartesian coordinates (Chassignet et al., 1996). Furthermore, the association of vertical shear with isopycnal packing and tilting in the ocean makes isopycnic models appropriate for studies of strong baroclinic currents, such as the Gulf Stream.

In the following experiments the vertical density structure is defined by 15 isopycnic layers, with sigma–theta values of 24.70, 25.28, 25.77, 26.18, 26.52, 26.80, 27.03, 27.22, 27.38, 27.52, 27.64, 27.74, 27.82, 27.88, and 27.92, topped by a dynamically active Kraus–Turner surface mixed layer. The vertical discretization was chosen in order to provide greater resolution in the upper ocean. The horizontal grid is defined on a Mercator projection, with the grid interval (in degrees) fixed in the longitudinal direction but varying with the cosine of latitude (Bleck et al., 1992).

The bottom topography is derived from a digital terrain data set with 5′ latitude–longitude resolution (ETOPO5) by averaging the topographic data located in each grid box. No additional smoothing was performed. The model is driven by atmospheric forcing fields based on monthly climatologies derived from the Comprehensive Ocean–Atmosphere Data Set (COADS) (da Silva et al., 1994). The momentum forcing is given by the longitudinal and latitudinal components of the wind stress, and the mixed layer stirring rate by the oceanic friction velocity. Thermal forcing is linearized (da Silva et al., 1994) around climatological SST (T_{clim}), in order to represent the model SST (T_{mod}) feedback on the surface heat fluxes, as:

$$Q = Q_{\mathrm{net}} + \frac{\mathrm{d}Q}{\mathrm{d}T_{\mathrm{clim}}}(T_{\mathrm{mod}} - T_{\mathrm{clim}}), \tag{1}$$

where Q_{net} and $\mathrm{d}Q/\mathrm{d}T_{\mathrm{clim}}$ are the time- and space-dependent net heat flux and restoring strength climatological fields, respectively. Fresh water fluxes (I) are specified as virtual salts fluxes based on the climatological evaporation (E) and precipitation (P) fields (independent of the model solution), as:

$$I = \frac{-S_{\mathrm{o}}(E - P)}{\alpha}, \tag{2}$$

where S_{o} is a reference salinity, and α is the specific volume of sea water. The northern and southern boundaries are closed, but are outfitted with 3° wide buffer zones (or sponge layers) in which salinity and layer interface depth are relaxed towards monthly values derived from the Levitus (1982) climatology. This procedure in the isopycnic

model is analogous to the relaxation to salinity and temperature in level models as long as the climatological and model vertical density gradients are sufficiently close to one another (Killworth, 1999). The restoring time scales vary linearly from 30 to 5 days from the inner to the outer edges of the buffer zones. The Mediterranean Sea is not included in the model domain, which is closed at the Straits of Gibraltar. Relaxation to climatology, with a time scale of 60 days, is applied in the Gulf of Cádiz in order to represent the outflow of salty Mediterranean waters into the Atlantic.

Subgrid-scale mixing is parameterized as proportional to the grid size (Δx), and momentum, thickness, and temperature/salinity diffusion coefficients are expressed as $u_d \Delta x$ (Bleck et al., 1992). The diffusion velocity u_d has values of 1.0, 0.2, and 0.5 cm/s in the 0.5° experiments, and 2.0, 0.5, and 1.0 cm/s in the 1° experiments, for momentum, thickness, and temperature/salinity, respectively. Mixing of momentum is enhanced in zones of strong horizontal shear, as a function of the deformation tensor (Smagorinsky, 1963; Bleck et al., 1992), with a proportionallity factor of 0.1 in the 0.5° experiments and 0.5 in the 1° experiments. The diapycnal mixing coefficient is $10^{-3}/\mathrm{N}$ $\mathrm{cm}^2\ \mathrm{s}^{-2}$ for all experiments, where N is the Brunt–Väisälä frequency.

The configurations of the various experiments are described below and are summarized in Table 1. The first experiment (Exp. L1.0) is run in a ''large'' CME-like domain (28°S to 65°N, including the 3° buffer zones), covering the equatorial, subtropical, and subpolar regions, with horizontal grid size of 1°. All subsequent experiments are run in a ''small'' (DAMÉE-NAB) domain, covering the North Atlantic subtropical gyre, from 6° to 50°N (including the 3° buffer zones). Two experiments are performed with the same 1° horizontal resolution as in Exp. L1.0: Exp. S1.0 with, and Exp. S1.0nr without, the restoring forcing applied at the lateral boundaries. Resolution is then increased to 0.5° in Exp. S0.5 and Exp. S0.5nr, with and without the restoring forcing applied at the lateral boundaries. The final experiment (Exp. S0.5sat) has the same configuration as Exp. S0.5, except that the SST field used in the heat forcing formulation (Eq. 1) is now derived from the satellite-based climatology.

The initial mass field is based on the Levitus (1982) January climatology for temperature and fall climatology for salinity (note that Levitus defines the fall season as November through January). For all experiments, the model was spun up from the rest for 7 years. Integrations were then carried out for an additional 3 years, for which the results were saved every 10 days and averaged to generate the model climatological

Table 1
Description of the model experiments. The domain limits in the table include the 3° wide buffer zones. The last column refers to the SST field used in the surface heat flux formulation in Eq. 1

Exp.	Grid size	Domain	Restoring at buffer zones	Surface forcing
L1.0	1°	28°S to 65°N	yes	COADS SST
S1.0	1°	6°S to 50°N	yes	COADS SST
S1.0nr	1°	6°S to 50°N	no	COADS SST
S0.5	0.5°	6°N to 50°N	yes	COADS SST
S0.5nr	0.5°	6°N to 50°N	no	COADS SST
S0.5sat	0.5°	6°N to 50°N	yes	SATELLITE SST

fields. Unless otherwise specified, the resulting model fields presented hereafter refer to this 3-year average, and are computed over the latitudinal band 9°N to 47°N (corresponding to the DAMÉE-NAB domain without the buffer zones). Exp. L1.0 was further integrated until year 20 in order to quantify the adjustment observed during the first 10 years.

3. Spin up of the simulations

In all experiments, the geostrophic adjustment to the initial climatological mass field leads to a rapid development of the wind- and thermohaline-driven circulations and the establishment of relatively strong surface and deep western boundary currents. After less than a month of integration, both Exps. L1.0 and S1.0 reach similar levels of total kinetic energy within the subtropical domain (Fig. 1), with Exp. L1.0 exhibiting larger maxima in the seasonal fluctuations after 5 years. In both cases, a multi-year period oscillation around the mean value can be observed [primarily confined to the upper layers (not shown)], suggesting an adiabatic adjustment associated with the westward propagation of the first baroclinic mode of Rossby waves. In the additional 10 years of simulation performed in Exp. L1.0 (years 10–20), the amplitude of this oscillation is reduced, indicating that a major adjustment of the circulation is indeed achieved in the first 10 years of integration. The third curve that appears in Fig. 1 pertains to Exp. S0.5 and illustrate the impact of higher resolution and lower dissipation. Most of the increase in total kinetic energy (roughly a factor of 2), when compared to that of the coarser resolution runs, is related to the intensification of the surface currents.

The model spin up is also dependent upon diabatic water mass transformations occurring within the mixed layer and inside the buffer zones. A long time scale adjustment of the baroclinic field is expected (Bryan, 1984), since the initial fields derived from climatology are not totally consistent with the forcing at the boundaries.

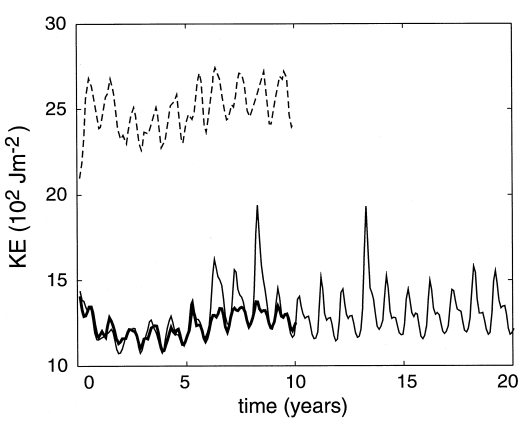

Fig. 1. Time evolution of the total kinetic energy integrated from 9°N to 47°N: Exp. L1.0 (thin solid line), Exp. S1.0 (thick solid line), Exp. S0.5 (dashed line).

Changes in the water masses within certain density classes are reflected in the simulations by changes in the volume of the model layers. A useful bulk index, representative of the diabatic adjustment in a layer model, is the domain-averaged layer thickness of each model layer (which represents the volume occupied by the layer, when multiplied by the domain area), the time evolution of which is presented in Fig. 2 for both Exps. L1.0 and S1.0. The annual cycle observed in layers 2 to 11, which is out of phase with the variations in the mass (or depth) of the mixed layer, reflects the ventilation of the subtropical gyre. The amplitude and phase of the annual cycle are in good agreement between the two experiments. Diabatic changes occurring outside the subtropical domain (mainly within the buffer zones) lead to a heating trend in the subtropics in both experiments, as mass is transferred from the deepest and coldest layers (15 and 16) to the warmer upper layers. While this trend is somewhat stronger in

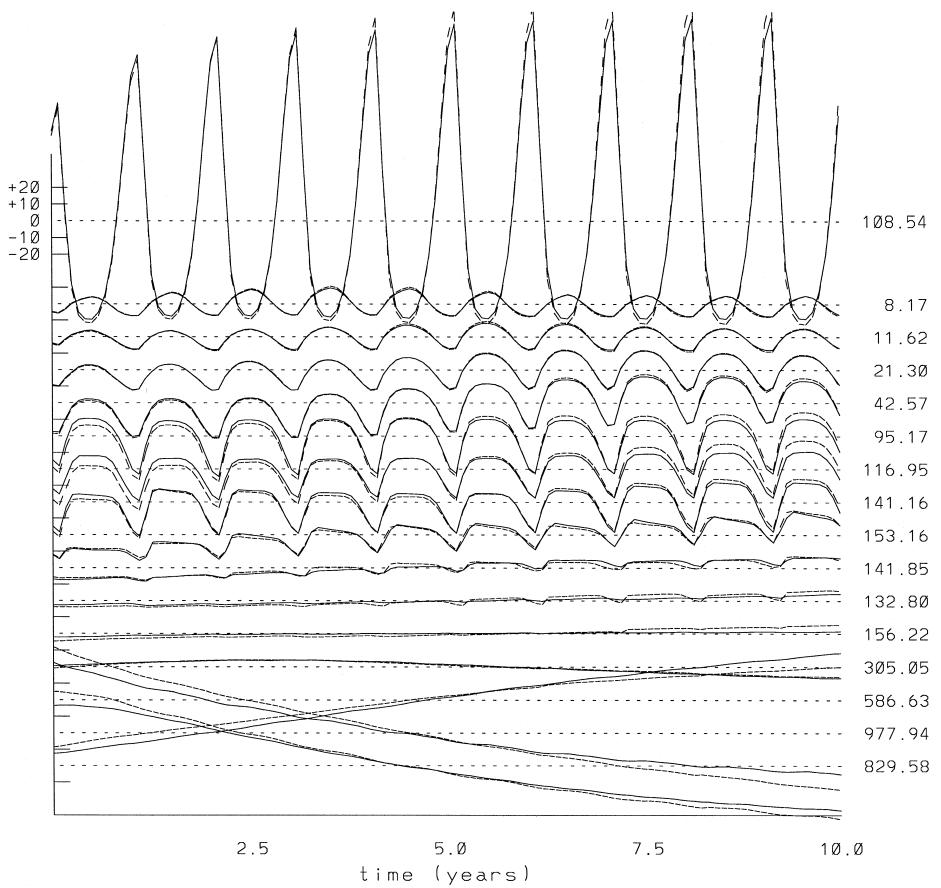

Fig. 2. Time evolution of the model average (9–47°N) layer thickness anomaly (the tick mark interval on the ordinate is 10 m): Exp L1.0 (dashed lines), Exp S1.0 (solid lines). The values at the right of the curves indicate the basin time averaged thickness of each layer.

Exp. L1.0 than in Exp. S1.0, the two cases are not significantly different by the end of the simulations.

The model adiabatic adjustment is not expected to be strongly constrained by domain size or by the position of zonally oriented boundaries, since the initial geostrophic adjustment is dependent basically on the oceanic climatology, and since Rossby wave propagation is primarily zonal. The same expectation is true for diabatic transformations associated with the ventilation of the main thermocline, as long as the circulation patterns and surface temperatures and salinities in the subtropical gyre are similar for the different domains. A remarkable result, however, is that buffer zones located near the limits of the subtropical gyre (the DAMÉE-NAB domain of Exp. S1.0) produce diabatic changes in the subtropical region comparable to those produced in the extended CME-like domain (Exp. L1.0), despite the fact that the restoring forcing in each case acts upon different horizontal mass fluxes, and upon different water mass properties.

Increasing the model horizontal resolution from 1° to 0.5° in Exp. S0.5 means that the diabatic processes within the boundaries occur in a larger number of grid points (since the width of the buffer zones is constant in all experiments), therefore possibly changing the efficiency of the buffer zones in generating mass conversions between the model layers (Beckmann et al., 1994). The adjustment of the mass field is not strongly affected by the increase in resolution, and the time evolution of the subtropical domain average layer thickness in Exp. S0.5 (not shown) follows closely those of Exps. L1.0 and S1.0 seen in Fig. 2. A similar result was obtained by Smith et al. (2000), when increasing resolution from 0.9° to $1/3°$ in simulations configured in a CME-like domain and with 4° wide buffer zones, although more significant changes were observed when resolution was increased in experiments with narrower buffer zones ($4/3°$). The fluxes of mass, heat, and salt generated by the lateral boundary conditions and the meridional transports are, however, modified by the change in resolution.

The time evolution of temperature averaged over the subtropical domain is shown for Exps. L1.0, S1.0, and S0.5 in Fig. 3 (upper panel), as a proxy for the change in the heat content. During the 10 year integration, the average temperature in Exp. S1.0 (Exp. L1.0) increases by ~ 0.2°C (~ 0.3°C), indicating an average heat gain at a rate of ~ 0.30 PW (~ 0.45 PW). This heat gain is due primarily to a lateral heat convergence (related to heat fluxes through the inner edges of the buffer zones) and is associated with the adjustment of the Meridional Overturning Cell (MOC). At the surface, the model loses heat to the atmosphere at a rate of ~ 0.35 PW, comparable to that observed (~ 0.40 PW computed from COADS). At the end of the simulations, the temperature curve flattens in Exp. S1.0, as a balance between the lateral and surface fluxes is reached, while the continuous temperature growth in Exp. L1.0 reflects the higher heat convergence observed in the Exp. L1.0 meridional heat transport (as discussed in Section 4). In Exp. S0.5, the average temperature still shows an increasing trend by the end of the simulation (Fig. 3), in contrast to the flattening of the temperature time evolution curve observed in Exp. S1.0. The reason for this behavior lies in part in the surface heat fluxes. While surface heat flux climatologies indicate an annual net loss of heat to the atmosphere of ~ 0.40 PW in the subtropical gyre, by the end of the simulation Exp. S0.5 loses only ~ 0.25 PW. This anomalous surface heating is through the oceanic feedback term in Eq. 1, and indicates that the model SST is lower, on

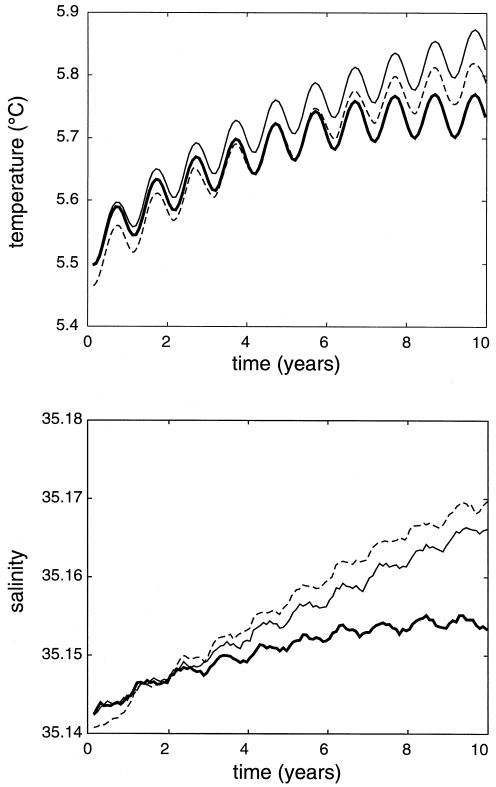

Fig. 3. Time evolution of the model averaged (9–47°N) temperature (upper panel) and salinity (lower panel): Exp. L1.0 (thin solid line), Exp. S1.0 (thick solid line), Exp. S0.5 (dashed line).

average, than the climatological SST. Most of this anomalous cooling of the model surface temperatures occurs in the spring, following the time when the mixed layer reaches its maximum depths. These depths are overestimated in the model, and the cooling results from a larger than realistic entrainment of cold waters at the base of the mixed layer.

In the interior constant density layers of the MICOM version 2.7 used in this study, only salinity is treated as a prognostic variable, and temperature is diagnosed. Consequently, the heat evolution in the model reflects to some extent that of the salt content, and the time evolution of the salinity averaged over the subtropical domain (Fig. 3, lower panel) shows a flattening in Exp. S1.0 and a continuous growth in Exp. L1.0 similar to those seen for temperature. In Exp. L1.0, the ~ 0.024 psu increase in the average salinity observed in the 10-year run corresponds to an average salt input of 8.5×10^6 kg/s, or, equivalently, to a fresh water loss of 0.24 Sv (1 Sv $\equiv 10^6$ m^3/s). When compared to the 0.6 Sv of annual net fresh water loss due to the excess of evaporation over precipitation computed from climatology, this indicates that the boundaries supply only $\sim 60\%$ of the observed fresh water input to the subtropics. The

increase in the average salinity is more pronounced in Exp. S0.5 than in Exp. S1.0, and the salinity time evolution curve in the former does not exhibit the flattening observed by the end of the simulation in the latter (Fig. 3). This behavior in Exp. S0.5 is associated primarily with an anomalously high inflow of salt through the Mediterranean buffer zone. The latter is further illustrated by comparing the domain averaged vertical temperature and salinity profiles from the Levitus and model climatologies in Fig. 4. The mismatch between the excess of evaporation over precipitation in the subtropics and the lateral freshwater fluxes is particularly strong at the surface, where the greatest increases in salinity (and differences between Exps. S1.0 and L1.0) are seen. At depths around 1000 m, salinity is lower in all experiments than in climatology (corresponding to a downward displacement of the isopycnals, as temperature changes are small). These differences are related to the representation of the Mediterranean outflow. Below 1500 m, salinity (and temperature) are greater in all experiments than in climatology.

Since one cannot appropriately model the Straits of Gibraltar with the chosen horizontal grid resolution, the outflow of Mediterranean waters into the North Atlantic is simulated by restoring the water mass properties to climatological values in a small buffer zone located in the Gulf of Cádiz. The limitation of this approach, however, is the same as at the northern and southern model boundaries, i.e., that the efficiency of this boundary condition is constrained by the flow generated by the model within the buffer zone. In order to evaluate the efficiency of this sponge layer in generating the appropriate flux of salt into the North Atlantic, it is useful to first consider some observational background. Waters with high salinity from the Mediterranean Sea flow into the Gulf of Cádiz, mix with the overlying waters, and then circulate and are subjected to further mixing in the North Atlantic. The signature of the Mediterranean outflow can be followed in observations across the subtropical gyre, up to the western basin, as a salinity maximum at depths around 1000 m (Arhan, 1987). A comprehensive

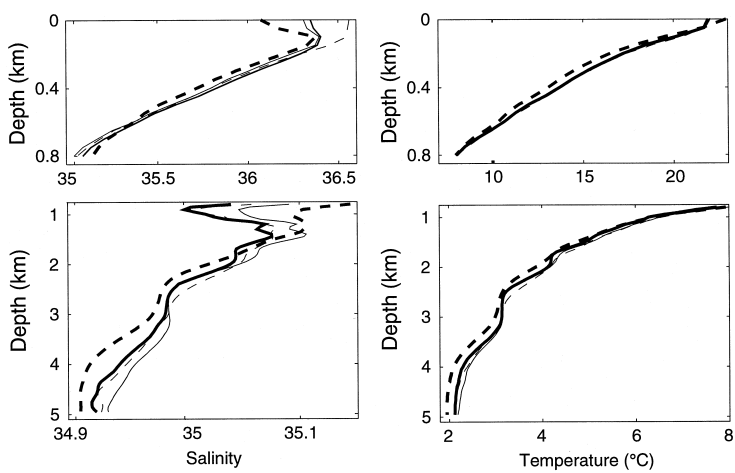

Fig. 4. Vertical profiles of area averaged (9–47°N) salinity (left) and temperature (right): Exp. L1.0 (thin solid line), Exp. S1.0 (thick solid line), Exp. S0.5 (thin solid line), Levitus (1982) climatology (thick dashed line).

view of the outflow and mixing of the Mediterranean waters has been given by Baringer and Price (1997). The source Mediterranean water, with $S \geq 38.4$ and $\sigma_\theta \geq 28.95$, flows through the Straits of Gibraltar into the Gulf of Cádiz as a bottom current. There, mixing with the fresher North Atlantic Central Waters (NACW) generates a neutrally buoyant water at depths near 1000 m, with $36.35 \leq S \leq 36.65$ and $27.3 \leq \sigma_\theta \leq 27.7$. This water then leaves the Gulf of Cádiz through its northern part and flows into the North Atlantic.

A vertical salinity section at 37°N, computed from the model climatology of Exp. S0.5, is presented in Fig. 5, and is compared to a section derived from the Levitus climatology. In contrast to observations, which indicate a salinity maximum (or intrusion) at mid-depths, the salinity structure in the model has been partially homogenized near the eastern boundary, around values of 35.6 psu (lower than observed). Time evolution plots of salinity near the Gulf of Cádiz (not shown) indicate that this decrease

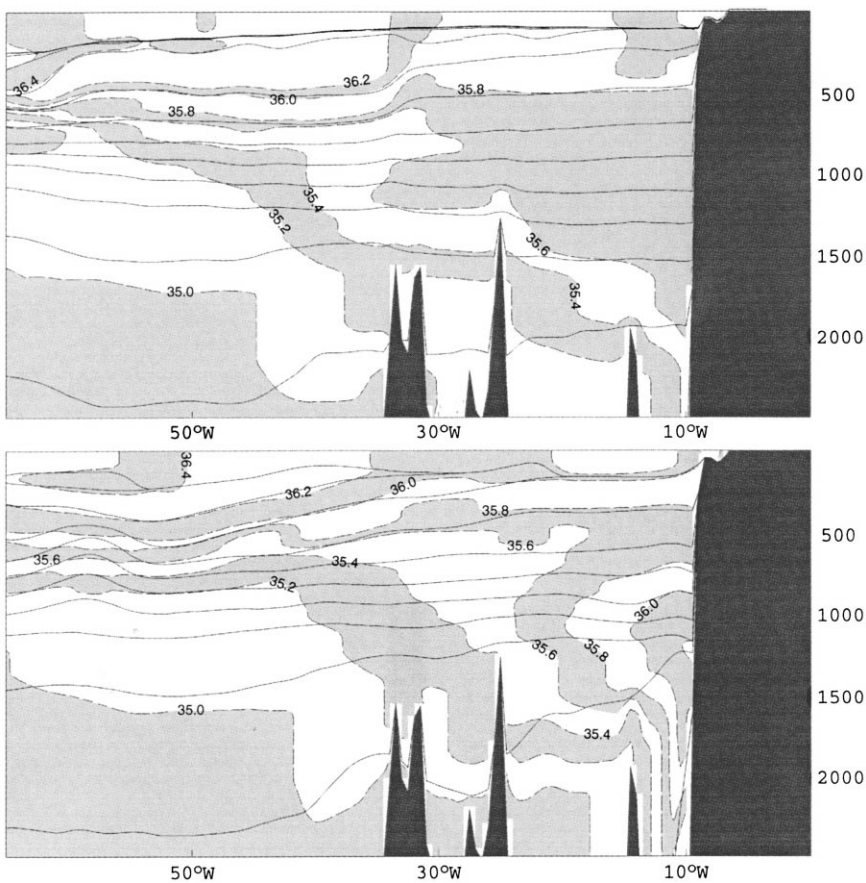

Fig. 5. Zonal sections along 37°N representing: (upper panel) salinity from the model climatology of Exp. S0.5; and (lower panel) initial condition salinity of Exp. S0.5 [based on Levitus (1982)]. Also shown are the model layer interfaces.

in salinity is not a continuous trend during the integration time (which would eventually cause the disappearance of the salinity intrusion), but rather is evidence that the model

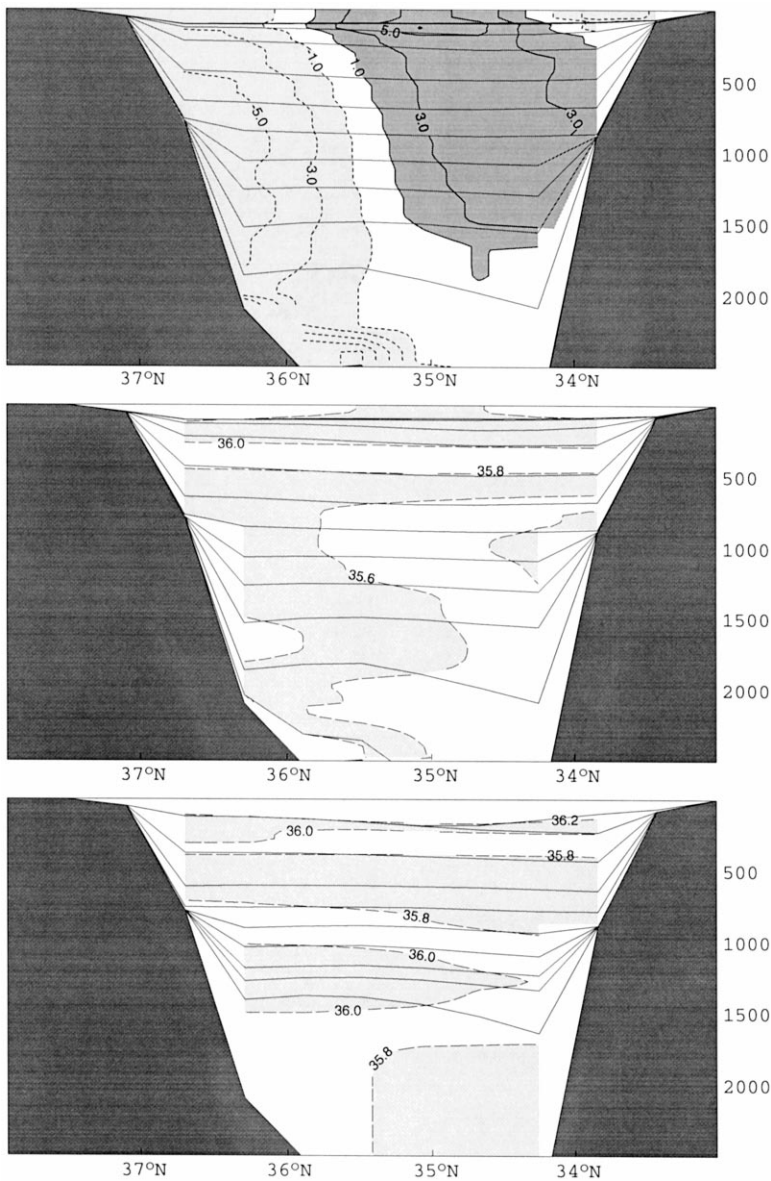

Fig. 6. Meridional sections along the edge of the buffer zone located at the Gulf of Cádiz. Velocity contours (cm/s) from the model climatology of Exp. S0.5 are shown in the upper panel, representing the flow into (solid lines with dark shading) and out of (dashed lines with light shading) the buffer zone. Salinity contours are shown in the middle panel for the model climatology, and in the bottom panel for the initial conditions [based on Levitus (1982)], of Exp. S0.5. Also shown are the model layer interfaces.

seeks an equilibrium state in which the mid-depth salinity intrusion is weaker than that in the observations. However, when the buffer zone at the Gulf of Cádiz is shut off, as in Exp. S0.5nr, the salinity intrusion disappears almost completely by the end of the simulation. The salinity intrusion in the North Atlantic is also considerably reduced in the 1° experiments that include relaxation in the Gulf of Cádiz. These results indicate that the relaxation boundary condition is capable of producing some Mediterranean water, although with lower salinity, and that the increase in the number of grid points in the sponge layer (which follows the increase in model resolution) plays a significant role in the efficiency of the restoring forcing in the Gulf of Cádiz.

Finally, in order to better understand what is accomplished by the Gulf of Cádiz buffer zone, velocity and salinity contours computed at the western edge of the Gulf (longitude 8.5°W) in Exp. S0.5 are shown in Fig. 6. A salinity section computed from the model initial state is also shown in the same figure for comparison. The inflow of fresher Atlantic waters at the edge of the buffer zone has a strong barotropic component, occupying the entire vertical column at the southern part of the Gulf of Cádiz. In Exp. S0.5, this barotropic flow is associated with the eastward flow of the model Azores Current (discussed in more detail in Section 5.3). Most of this flow turns northward in the Gulf of Cádiz and then westward into the interior Atlantic Ocean. The maximum flow out of the buffer zone occurs near the bottom, at depths around 1000 m, in agreement with observations reported by Baringer and Price (1997). As the fresher North Atlantic waters recirculate inside the Gulf, the salinity of the buffer zone in the outflow region is homogenized at ~ 35.6 psu (Fig. 6), which is a lower value than observations indicate and which corresponds to the average value of the salinity intrusion into the North Atlantic in the model.

The actual average flux of salt from the buffer zone into the North Atlantic in the models is $\sim 5 \times 10^6$ kg/s, corresponding to an equivalent fresh water loss to the Atlantic of ~ 0.13 Sv. This value is high when compared to an estimated fresh water flux of ~ 0.04 Sv through the Straits of Gibraltar, which is necessary to compensate for the excess of evaporation over precipitation inside the Mediterranean (Bryden and Kinder, 1991). The model salt flux into the Atlantic is overestimated by a factor of ~ 3, while the salinity of the outflowing waters is reduced. This can be explained by the barotropicity of the flow in the Gulf of Cádiz, which leads to high inflow and outflow volume rates. While ~ 20 Sv cross the edge of the Gulf of Cádiz at any time in the model, observations indicate a transport of only ~ 7 Sv (Ochoa and Bray, 1991).

4. Meridional overturning circulation and associated heat transport in the subtropical gyre

Overturning streamfunctions representing the MOC are shown in Fig. 7 in density space. As in previous simulations (Chassignet et al., 1996), MICOM produces a strong overturning, with maximum values at 24°N of about 20 Sv in Exp. S1.0 (middle panel). This value is within the observational range of 17 ± 4 Sv computed by Roemmich and Wunsch (1985) from oceanographic sections at 24°N, and within the estimated range of

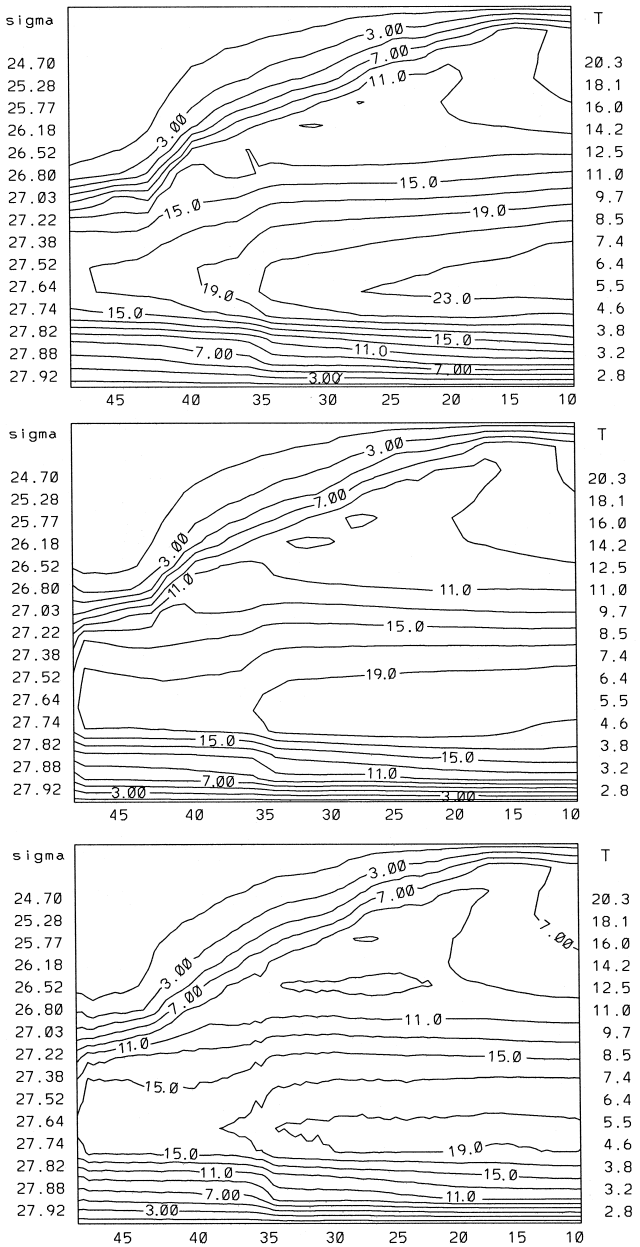

Fig. 7. Meridional overturning streamfunction in density space, (years 8–10): Exp. L1.0 (upper panel), Exp. S1.0 (middle panel), and Exp. S0.5 (lower panel). The values on the abscissa are latitudes, and the values at the right side of the plots represent the average temperature of each layer (computed for a constant salinity of 35 psu).

18–20 Sv for the net transport by the DWBC in the North Atlantic [consisting of 13 Sv of North Atlantic Deep Water (NADW) formed in high latitudes and 5–7 Sv of Antarctic Bottom Water (AABW) and Antarctic Intermediate Water (AAIW) contribution] given by Schmitz and McCartney (1993). By contrast, in Exp. L1.0 (Fig. 7, upper panel), the maximum overturning after 10 years of simulation reaches ~ 23 Sv close to the southern boundary. Although still within the range of some of the higher observational estimates [Broecker (1991), for instance, suggests that $\sim 20 \pm 5$ Sv are necessary to balance the budgets of radiocarbon tracers], this value in the model actually reflects the longer adjustment time of the overturning circulation in the large domain experiment. The adjustment is faster in higher latitudes (transports at the northern edge of the subtropical gyre are comparable to those found in the small domain experiment) and slower in southern latitutes. The transports in Exp. L1.0 will reach levels similar to those of Exp. S1.0 in low latitudes only by the end of year 20.

The pattern of the overturning streamfunction in Exp. S0.5 is very similar to that of the 1° case (Exp. S1.0), but the maximum transport is reduced by roughly 1 Sv throughout the domain (Fig. 7, lower panel). A similar decrease in the strength of the MOC with increased resolution was found in simulations with a depth coordinate model by Beckmann et al. (1994). Smith et al. (2000), however, in experiments with MICOM, found an increase in the strength of the MOC with increased resolution, the opposite behavior of the present simulations. Judging from these results alone, no simple rule can be postulated that determines the relationship between resolution and strength of the overturning circulation. Note, however, that none of these experiments has been carried out to equilibrium, inplying that the results may simply reflect only initial trends in the adjustment process.

Overturning plots in density space (a natural choice of coordinates in isopycnic models) lead to a clear visualization of the mass exchanges between density classes along the path of the MOC, since, for a stationary solution, ''vertical'' velocities in the plot translate into diapycnal fluxes. For non-stationary solutions, such as the ones discussed in this paper, these vertical velocities can also reflect changes in the volume of the model layers (Nurser and Marsh, 1998). The latter velocities are quite small since, in all experiments, the overturning streamfunctions computed in either density or depth coordinates are almost identical. Transports given in density coordinates can also be directly compared to observational estimates, which are reported in terms of transports within fixed density classes (e.g., Schmitz and McCartney, 1993; Schmitz, 1996). Note, however, that the model is discretized in σ_θ, and cannot resolve the AABW (Sun, 1998).

In Exp. S1.0, ~ 15 to 17 Sv circulate through the whole basin, interacting with both the northern and southern buffer zones (Fig. 7, middle panel). The cold branch of the overturning circulation, primarily the southward flow of the model Deep Western Boundary Current (DWBC), consists in the model of ~ 10 Sv transported in the two deepest layers ($\sigma_\theta \geq 27.88$ and average temperatures < 3°C) and ~ 6 Sv transported in the next two layers above ($\sigma_\theta = 27.74$ and 27.82 and average temperatures of ~ 3–4°C). Within the constraints of the model vertical resolution, these figures are in good agreement with those of Schmitz and McCartney (1993), who suggest that there is an outflow of ~ 16 Sv from subpolar to subtropical regions, consisting of 12 Sv of lower (1.8–3°C) and 4 Sv of upper (3–4°C) NADW.

The upper branch of the overturning represents primarily waters that upwell in southern latitudes (accomplished in the model inside the narrow southern buffer zone) and return as a warm northward flow. In Exp. S1.0, ~6 Sv enter the subtropics from the southern buffer zone at the surface ($T \geq 24°C$) and are transported within the mixed layer, cooling (and moving down in density space) on their way north via the western boundary currents. A net transport of ~4 Sv occurs in a wide range of temperatures (12–24°C at the southern boundary) corresponding to upper thermocline waters (note the spacing of the transport streamfunction contours in Fig. 7). Finally, ~6–7 Sv are transported in the temperature range from 7–12°C, flowing along the western boundary into the Caribbean Sea and joining the Florida Current. At the latitudes of the Gulf Stream, most of the warm flow interacts with the atmosphere through the mixed layer, where it is cooled and made denser. This pattern of transport in the upper branch of the overturning circulation in the model is similar in many aspects to that presented by Schmitz and McCartney (1993) in a compilation from observational evidence. The most significant difference between the model and observations is that, in the latter, the net transport through the upper thermocline is very small (~1 Sv). Consequently, the warm return flow adds up to only ~13 Sv in the observational scenario, and the additional 3 Sv needed to balance the southward transport is attributed to upwelling of AABW into the NADW, a water mass not represented by the model's vertical discretization in σ_θ.

Part of the flow generated in the southern buffer zone in Exp. S1.0 (~2 Sv) does not reach the northern boundary, but recirculates inside the domain in the temperature range of roughly 4–7°C (Fig. 7, middle panel). The warmer branch of this flow, centered on $\sigma_\theta = 27.38$ in the model, corresponds to the AAIW that flows along the western basin up to latitudes between 35° and 40°N, where it is converted into denser layers and returns southward as part of the DWBC. The influence of AAIW in the Gulf Stream region has been detected in observations by Richardson (1977) and Tsuchiya (1989), and its sinking

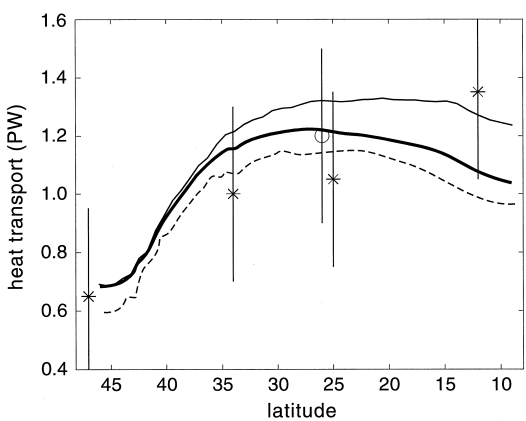

Fig. 8. Model meridional heat transport (years 8–10): Exp. L1.0 (thin solid line), Exp. S1.0 (thick solid line), and Exp. S0.5 (dashed line). The circle is the value proposed by Hall and Bryden (1982), based on observations, and stars are values from the inverse computation of Macdonald and Wunsch (1996). Vertical lines are the error bars of each estimate.

and modification into upper NADW have been hypothesized by Schmitz and McCartney (1993).

The meridional heat transport (which is primarily associated with the MOC) is shown in Fig. 8 for the various experiments and is compared to observations. The canonical value of meridional heat transport, to which most numerical studies are generally compared, is 1.2 ± 0.3 PW at 24°N, computed from direct oceanographic observations by Hall and Bryden (1982). Also shown in Fig. 8 are the inverse calculation values of Macdonald and Wunsch (1996). Model results are within the observational range in mid-latitudes, and the transport at 24°N in Exp. S1.0 agrees remarkably well with the estimate from Hall and Bryden (1982). The heat transport in Exp. L1.0 is greater than that in Exp. S1.0 (especially towards lower latitudes), reflecting the stronger MOC in the former, and is in close agreement with the estimate of Macdonald and Wunsch (1996) at 11°N. However, the heat convergence between 10°N and 25°N associated with the latter estimate implies a significant heat loss by the atmosphere, in disagreement with most heat flux climatologies for this region (Large et al., 1997). The decrease in the meridional heat transport (1.1 PW at 26°N) in Exp. S0.5, when compared to that of Exp. S1.0, mirrors the decrease in the MOC strength (Fig. 7, lower panel).

5. Surface circulation

5.1. Large versus small domain

The surface velocity climatology of Exp. L1.0 is shown in Fig. 9 (upper panel), representing the mean wind-driven gyres of the equatorial, subtropical, and subpolar regions. As a typical result of the viscous solutions obtained with medium resolution grids, the major currents are broad and stable, and the Gulf Stream overshoots its separation point at Cape Hatteras. Another aspect characteristic of the medium resolution is the poor representation of small islands and narrow passages that constrain the flow of oceanic currents. The Antilles, for instance, are ''seen'' by the model only as a general elevation of the local topography, and the tropical western boundary current flows unconstrained into the Caribbean Sea as a relatively strong zonal jet. In the Florida Straits, the small number of grid points limits the flow of the Florida Current to only ~ 10 Sv (Chassignet et al., 1996), and results in the merging of the Florida and Antilles Currents into a single broad northward flow.

Also shown in Fig. 9 (upper panel) are the limits of the small domain case (Exp. S1.0), including the northern and southern buffer zones. As seen in the figure, there is substantial inflow and outflow through these boundaries in the western basin. In the small domain case, this inflow must be generated and the outflow absorbed by the sponge layers. The surface velocities of Exp. S1.0 are shown in Fig. 9 (middle panel), and the flow pattern and transports in the subtropical gyre are very similar to those of Exp. L1.0. At low latitudes, the seasonal cycle (not shown) of the equatorial currents is well represented in the small domain, including the simulation of an Equatorial Counter Current in the summer and fall (primarily inside the buffer zone). At the South American coast, the Guyana Current emerges from the sponge layer as a continuous

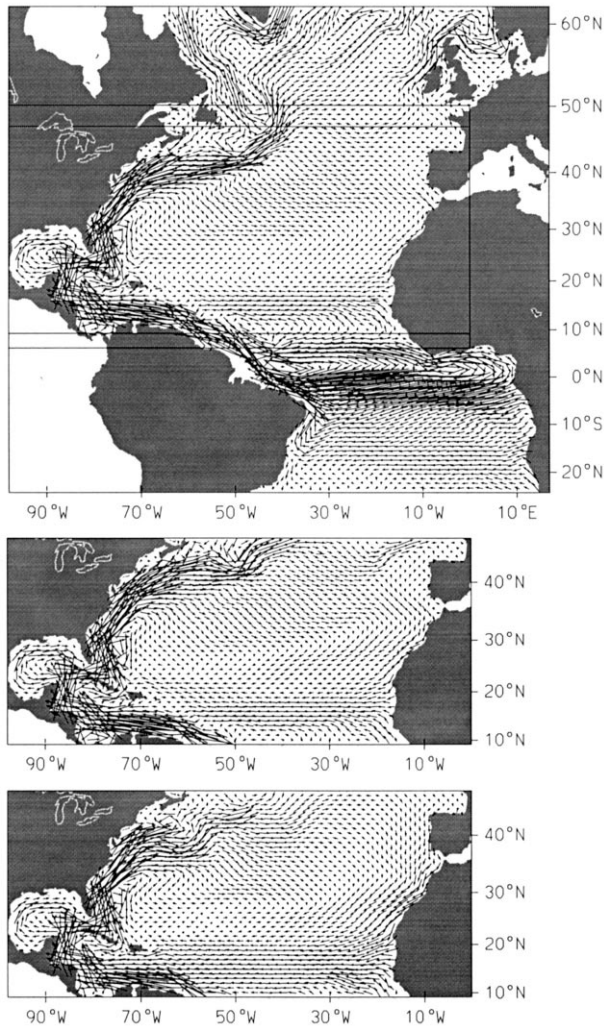

Fig. 9. Model surface velocity climatology: Exp. L1.0 (upper panel), Exp. S1.0 (middle panel), and Exp.S1.0nr (lower panel). Maximum Gulf Stream velocities on the order of 25–30 cm/s. The model domain and buffer zones in Exps. S1.0 and S1.0nr are also shown in the upper panel, to facilitate the comparison between the experiments.

flow, with similar horizontal and vertical structure (not shown) to those of the larger domain case. Recent observational studies, however, suggest that in reality, the Guyana Current exists only in an average sense, as a rectification of the northwestward propagating North Brazil Current rings (Richardson et al., 1994). Such rings are not formed in the present simulations due to the low horizontal resolution and the upper branch of the model thermohaline circulation is therefore represented by a continuous current.

At the northern boundary, a southward flow can be observed in the shallow waters of the Grand Banks in both model cases. While in Exp. L1.0 this flow is a continuation of the Labrador Current, which is the western branch of a well developed cyclonic subpolar gyre in the model, in Exp. S1.0 it is generated solely inside a small part of the model domain and of the buffer zone. In both simulations, this flow acts as a source of cold waters to the Grand Banks region, creating a thermal front along the path of the Gulf Stream, along which subsurface layers outcrop. The Gulf Stream follows basically the

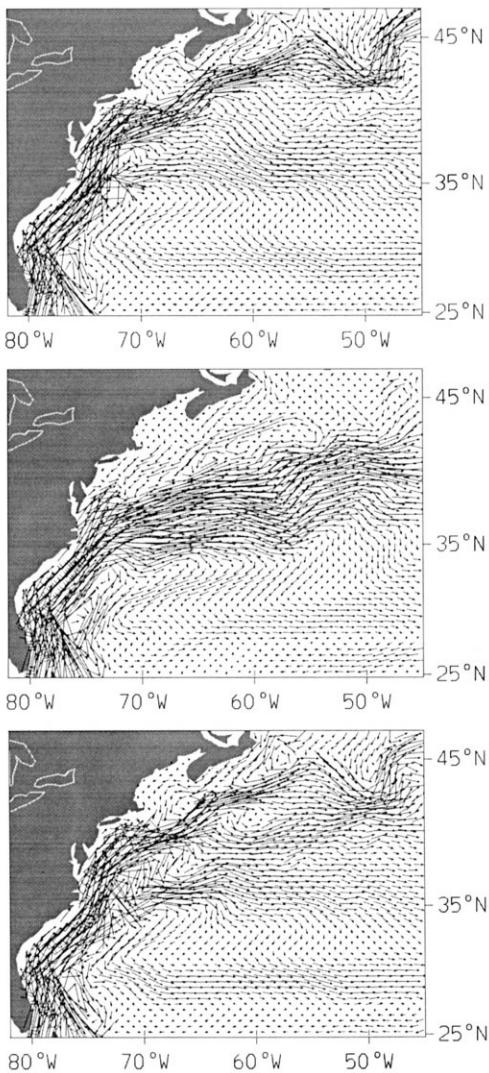

Fig. 10. Model surface velocity climatology in the Gulf Stream region: Exp. S0.5 (upper panel), Exp. S0.5nr (middle panel), and Exp. S0.5sat (lower panel). Maximum Gulf Stream velocities on the order of 55–60 cm/s.

same path in both experiments — note that the current flows into the northern buffer zone in Exp. S1.0 at approximately the same longitude at which it flows into the subpolar region in Exp. L1.0. However, there is a slight intensification of the zonal flow in the northeast subtropical gyre in Exp. S1.0, when contrasted to the flow in that region in Exp. L1.0. The narrow sponge layer is not able to accommodate all the flow from the Gulf Stream, and a small part of it is forced to recirculate inside the domain.

The buffer zone approach primarily allows the model to represent the vertical water mass conversions responsible for the thermohaline-driven circulation. The surface velocities in the subtropical gyre derive from a combination of the wind-driven circulation plus a northward flow (mainly along the western boundary) corresponding to the warm branch of the overturning cell (Schmitz and McCartney, 1993). A third experiment was performed in order to verify the impact of the mass conversions within the buffer zones upon the surface circulation. Exp. S1.0nr (Fig. 9, lower panel) was carried out with the same configuration as Exp. S1.0, but without the restoring adjacent to the lateral walls. In this case, the northwestward flow along the South American coast is intermittent, and exists only as a continuation of the North Equatorial Current, which reaches the coast in the periods when the tropical gyre recedes southward. There is also no inflow of cold waters at the northern boundary into the Grand Banks, and the thermal front observed in the experiment with the restoring force (Exp. S1.0) disappears. The Gulf Stream still overshoots its separation point at Cape Hatteras, but its subsequent path is modified and does not converge toward the northern boundary. Most of the flow is then forced to recirculate inside the domain, eventually enhancing the meridional flow in the eastern basin and affecting the Equatorial currents.

Increasing the model horizontal resolution from 1° to 0.5° in the small domain configuration (Exps. S1.0 and S0.5) reveals a more complex picture of the surface circulation, in which the broad flows of the coarser simulations are replaced by narrower surface jets. Specific examples are the intensification of the surface velocities associated with (a) the wind-driven zonal flow associated with the C-shaped form of the Sverdrup solution in the western basin (Fig. 10) and (b) the model representation of the Azores Current in the eastern basin (discussed in Section 5.3).

5.2. Gulf Stream representation

As mentioned in the previous section, the specification of the lateral boundary conditions does exert an impact on the Gulf Stream path. In Exps. L1.0, S1.0, and S0.5, the Gulf Stream overshoots its separation point and follows an unrealistic northward path along the coast (Fig. 9, upper panel of Fig. 10). The increase in resolution in Exp. S0.5, however, induces part of the western boundary current to separate from the coast at Cape Hatteras. In Exp. S1.0nr, in which no restoring to climatology is applied at the lateral walls, the simulated path is zonal eastward of $\sim 70°$W (Fig. 9) and shows a tendency to separate from the coast. In the same experiment but with increased horizontal resolution (Exp. S0.5nr), the Gulf Stream behavior is further modified with a more realistic separation and path, following the mean zero wind stress curl line (Fig. 10, middle panel), and with the establishment of a barotropic cyclonic circulation north

of the Gulf Stream, the signature of which can be seen in the surface velocities in Fig. 10. The reason for this behavior is not clear, but the overshooting in the experiments with boundary restoring may simply reflect the interaction of a relatively weak wind-driven surface current with a relatively strong thermohaline-driven northward flow corresponding to the warm branch of the overturning circulation. While the former tends to follow the zero wind stress curl line and separate at Cape Hatteras, the latter hugs the coast as a western boundary current, displacing the Gulf Stream northward.

Associated with the overshooting of the Gulf Stream in Exps. L1.0, S1.0, and S0.5, there is a northward displacement (when compared to observations) both of the SST

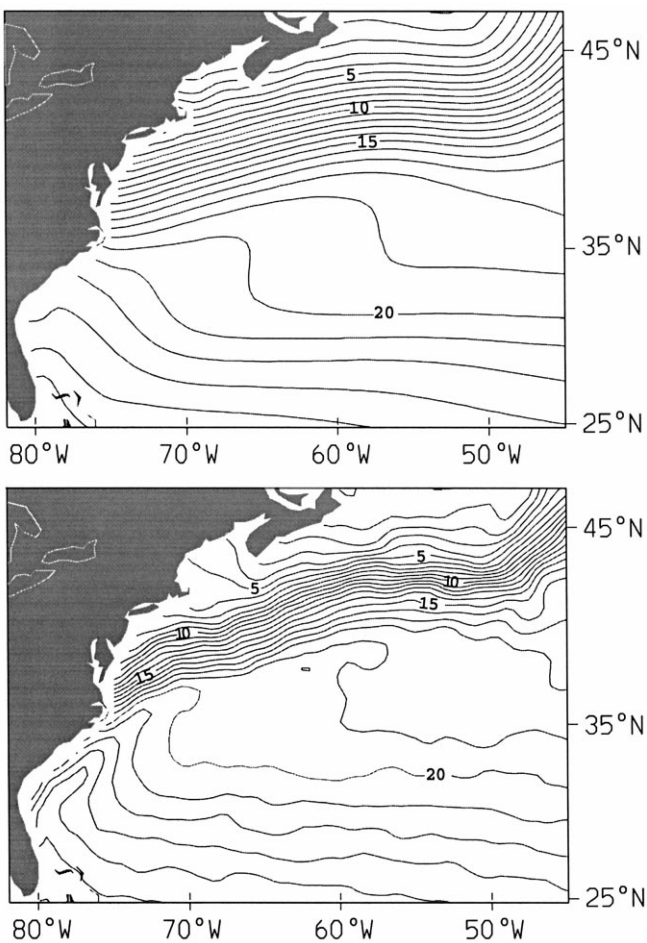

Fig. 11. Sea surface temperature in the Gulf Stream region. The upper pannel represents the COADS climatology, derived from ship based observation; the lower panel represents the climatology created by the Remote Sensing Group at the University of Miami, and derived from AVHRS satellite observations. The latter has a better resolution on the thermal front associated with the Gulf Stream, for the entire year (only the April SST climatologies are shown).

front along the axis of the current and of the outcropping line of the thermocline layers. The importance of preserving the thermal (or density) structure of the slope waters for achieving a realistic separation has been emphasized by Ezer and Mellor (1992). Analytical studies by Nof (1983) and Nurser and Williams (1990) also showed that surface cooling can lead to a southward migration of the separation point. The COADS SST climatology, which is used in the heat flux computation in the present simulations, is very smooth [due to the sparse (in space and time) ship based observations] and does not represent strong frontal systems well. In Exp. S0.5sat, we assess the impact upon the model circulation of a climatology based on AVHRR satellite observations, collected over a 5-year period (1987 to 1991), and objectively analyzed and interpolated to a 36-km grid by the Remote Sensing Group at the University of Miami. In addition to the increased spatial resolution, this climatology provides a better representation of oceanic fronts, such as in the Gulf Stream region (Fig. 11). In Exp. S0.5sat, the heat flux formulation of Eq. 1 was therefore modified by substituting the new SST climatology for the COADS SST climatology.

The resulting surface velocity climatology in Exp. S0.5sat is shown in the lower panel of Fig. 10, which can be compared to the results of Exp. S0.5 (upper panel of Fig. 10). The differences between the two experiments are not large, as the Gulf Stream still overshoots the observed separation point at Cape Hatteras, and the main branch of the current still flows along topography. There is however a significant intensification of the southern branch of the Gulf Stream, which separates at the latitude of Cape Hatteras. The signature of the stronger cooling in Exp. S0.5sat can also be seen in the stronger water mass conversions that occur in the Gulf Stream region, which are seen to reach the upper part of the DWBC in the overturning streamfunctions (not shown).

5.3. Azores current / Gulf of Cadiz circulation

The surface velocities in the eastern North Atlantic are shown in Fig. 12 for Exps. S1.0, S0.5, and S0.5nr. A distinguishable feature in Exp. S0.5 is the presence of a narrow zonal current that flows eastward near latitude 34°N as the model representation of the Azores Current (Fig. 12, middle panel). This flow can be recognized as a coherent zonal jet from $\sim 40°$W until it approaches the continental shelf ($\sim 10°$W), where part of the flow enters the southern region of the Gulf of Cádiz, and part turns to the south and feeds the Canary Current. In the 1° experiments, however, only a broad zonal flow exists between $\sim 40°$W and $\sim 20°$W, and the circulation is primarily meridional westward of $\sim 20°$W (Fig. 12, upper panel). In the following, model results are compared to observations, and the reasons for the different representations of the Azores Current resulting from the different model resolutions are investigated.

The primary source water for the model Azores Current is a southeastward flow located westward of $\sim 40°$W, which originates from the southern branch of the Gulf Stream extension. A similar connection between the Azores Current and the Gulf Stream has been established from observations (Klein and Siedler, 1989). In Exp. S0.5, the Azores Current reaches depths of ~ 1000 m over most of its extension, and has a vertical structure that is characterized, both in the model and in observations (Rios et al., 1992), by a salinity front and by the sloping of the isopycnals in the north–south

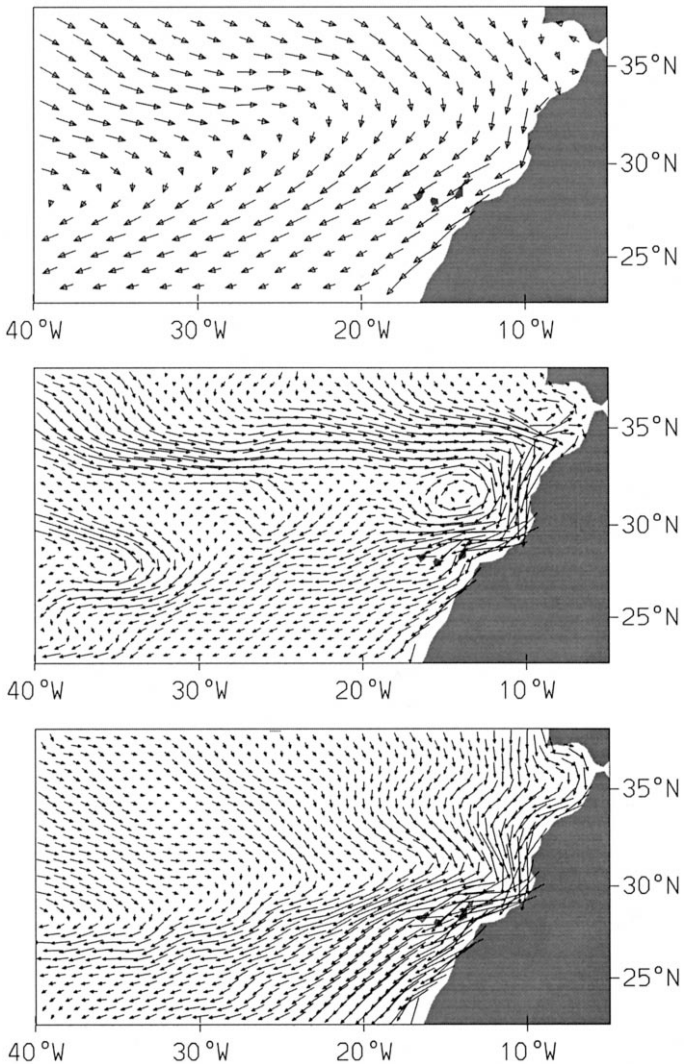

Fig. 12. Surface velocity climatology in the eastern basin: Exp. S1.0 (upper panel), Exp. S0.5 (middle panel), and Exp. S0.5nr (lower panel).

direction. Maximum model surface velocities on the order of 5 cm/s are low when compared to observed values of ∼15 cm/s, and the model current is very stable, in contrast to observations that show the Azores Current as an important source for the variability in the eastern North Atlantic (Brügge, 1995).

The reasons for the existence of the Azores Current are unclear (Spall, 1990). In an analysis of linear solutions obtained with a high resolution numerical model forced by various wind stress climatologies, Townsend et al. (2000) show that Sverdrup dynamics

account for only 1–2 Sv of the zonal flow in this region. The estimated transport from direct observations, however, is 11 ± 1.5 Sv (Stramma, 1984). In the present simulations, the zonal transport increases with the increase in resolution, from ~ 2.5 Sv in Exp. S1.0 to ~ 10 Sv in Exp. S0.5. The change in resolution in the model domain accounts for the observed narrowing and strengthening of the current, but it cannot account for such a difference in the volume transport. In order to investigate to what extent the different representations of the Azores Current in the present experiments are attributable to the effects of increased resolution inside the sponge layer located in the Gulf of Cádiz, the results of Exp. S0.5nr (which was carried out in the same configuration as Exp. S0.5 but with no relaxation in the buffer zones) are also analyzed.

Surface velocities in Exp. S0.5nr are shown in Fig. 12 (lower panel). The flow is primarily meridional near latitude 34°N in this case, and the simulation is unable to represent the Azores Current. The sequence of experiments shown in Fig. 12 (Exps. S1.0, S0.5, and S0.5nr) suggests that the existence of the Azores Current in the model is directly related to the water mass transformations that occur in the Gulf of Cádiz. A similar connection between the Azores Current and the relaxation in the Gulf has also been obtained by Jia (2000), in simulations performed in the context of the DYNAMO (1997) experiment. This idea was further explored by Özgökmen et al. (2000) in a series of idealized experiments, which showed that a sink corresponding to the entrainment of North Atlantic upper ocean water by the Mediteranean outflow can actually induce zonal flows resembling the Azores current in location and transport.

The different model resolutions also result in different representations of surface circulation to the south of the Azores Current and the Gulf of Cádiz (Fig. 12). In this area, the Canary Current can be observed as a relatively intense southward flow in the two 0.5° experiments (Exps. S0.5 and S0.5nr). Exp. S0.5 is more realistic than Exp. S0.5nr in representing the Canary Current, in the sense that the former preserves the connection between the Azores and the Canary Currents that is seen in observations (Stramma, 1984), and in the sense that the flow in the eastern basin in the latter is affected by the recirculation of Gulf Stream waters inside the domain (as discussed in Section 5.1).

6. Summary and discussion

A series of simulations have been carried out with the Miami Isopycnic Coordinate Ocean Model (MICOM) in the context of DAMÉE-NAB, in order to explore its capacity to reproduce the wind- and thermohaline-driven circulations in the North Atlantic subtropical gyre. This paper addresses the constraints imposed on the simulations by the domain size and by the position of the ocean lateral boundaries. These boundaries are closed in all simulations, but are outfitted with 3° wide buffer zones that seek to reproduce diabatic water mass transformations through a Newtonian relaxation of model properties towards oceanic climatologies.

Simulations performed in a large CME-like domain (28°S to 65°N) and a smaller DAMÉE-NAB domain (6°N to 50°N) have been compared. In the former configuration, the flow into the subtropics is related to the model circulation in the subpolar and

equatorial regions, but in the latter this flow depends solely on the interaction between the circulation in the subtropics and the restoring forcing at the boundaries. Klinck (1995), analyzing the CME simulations of Bryan and Holland (1989), observed that the flow through the edge of the buffer zones (defined as the sum of all positive or all negative meridional fluxes through the boundary) was two to eight times larger than that expected on the basis of observations. Klinck (1995) suggested that the additional transport might be related to recirculating cells established in the vicinity of the boundaries and driven by excessive vertical velocities within the buffer zones. This observation suggests that the inner edge of the buffer zones is simply an arbitrary location (and perhaps not the most appropriate) at which to separate, in the analysis of the model results, the internal domain (the region of interest) from the external forcing region, since undesirable processes related to the boundary forcing may extend into the domain from the buffer zones. In the present simulations, despite the fact that the boundaries in the small domain are located adjacent to the region of interest, and that these boundaries intersect strong meridional surface flows in the western basin (in contrast to the situation in the large domain), the restoring force is able to generate appropriate inflow and outflow conditions without significantly disrupting the circulation in the subtropical gyre. The flow into the subtropics (as defined above) in the small domain simulation was found to be only ~ 15–20% larger than that generated in the large domain simulation.

The transports and pathways associated with the thermohaline circulation, which is induced primarily at the lateral boundaries, were shown to compare well with observations, within the constraints of the model configuration. The discretization in density space is particularly suitable for such comparisons [see for instance Smith et al. (2000) and Sun (1998)], since the model layers can be configured to represent specific density classes depicting particular oceanic water masses. Northward of ~ 35–$40°$N, the meridional transports of mass and heat converge to near observational values in the first year of integration and vary little afterwards, in both the small and the large domain simulations. Southward of this latitude, however, the overturning streamfunctions depict an initially strong internal recirculating cell in the intermediate model layers, which decays with time during the integration. After 10 years, the values of maximum overturning strength and heat transport across the model domain are in good agreement with observations in the small domain simulations. In the large domain, however, the recirculation is more intense and, consequently, the overturning strength and heat transport in the southern portion of the subtropics are overestimated. Time series of the overturning strength at several latitudes in the model (not shown) reveal that the MOC adjustment occurs at similar rates during the simulation in both cases, and that the stronger MOC in the large domain is related to a stronger recirculation generated during the initial adjustment.

The diabatic processes occurring inside the southern buffer zone account for the upwelling and conversion of deep cold to intermediate and surface warm waters. The associated vertical motion, or, more appropriately in a layer model, the diapycnal fluxes within the boundary region, result mainly from a kinematic mode in which inflow and outflow associated with the climatological shear at the boundary requires vertical motion by continuity (Klinck, 1995). The same process is present in the northern boundary

region and is responsible for the formation of the bulk of NADW which in reality occurs in the Greenland and Denmark Seas via intense deep convection. In addition, convective processes are also responsible for some of the diabatic transformations taking place in the northern buffer zone. In the CME-like simulations, the northern boundary captures the properties of the deep water just below the outflow from the northern seas, and includes a portion of the Labrador Sea, in which deep convection generates waters of the upper branch of the DWBC. In the DAMÉE-NAB configuration, the boundary is located at the northern limits of the subtropical gyre, and convection within the sponge-layer accounts for a small part of the thermocline ventilation. Given these differences, it is notable that the best agreement in the overturning circulations produced by the small and large domains occurs in the northern latitudes of the subtropics.

The impact of grid resolution was assessed by refining the model horizontal grid from 1° to 0.5°. This implies an increase in the number of grid points inside the buffer zones (for a given width of the buffer zones) through which diabatic water mass conversions take place. Such an increase modifies the vertical mass transfer within the boundaries and consequently the efficiency of the buffer zones (Beckmann et al., 1994; Smith et al., 2000). This was shown to be particularly important for the sponge layer located in the Gulf of Cádiz to simulate the outflow of salty Mediterranean waters into the North Atlantic, which, under certain circumstances, can significantly modify the interior water mass properties. Furthermore, a connection between the transport and path of the model Azores Current and the restoring force in the Gulf of Cádiz was established, suggesting that the real-world Azores Current may owe its existence to the combined effects of wind forcing and of the circulation and water mass transformations within the Gulf of Cádiz, which are associated with the Mediterranean inflow/outflow.

Varying both the grid resolution and the restoring forcing at the boundaries also leads to diverging representations of the western boundary current, especially its separation from the coast. Understanding the dynamics of the Gulf Stream separation, its relationship to external forcing, and its interactions with bottom topography and deep flows has been the focus of many investigations. Recent results suggest that nonlinear dynamics, related to high reoslution in numerical models, must be invoked for a complete description of the problem. However, medium and coarse resolution models have proved to be useful tools, particularly when long term integrations are sought. Among the consequences of the typical overshooting observed in such models is the northward shift of the SST front associated with the Gulf Stream path, and therefore the generation of anomalous heat fluxes to the atmosphere. Consequently, obtaining the correct heat balance in ocean circulation models is directly related to achieving a correct representation of the separation. A significant part of the interannual and decadal SST variability in the North Atlantic has recently been associated with processes occurring at the Gulf Stream front (Joyce et al., 2000), and it is therefore important to understand the separation process in non-eddy-resolving simulations. An attempt to improve the separation, while preserving the thermal front associated with the Gulf Stream, was made in an experiment incorporating assimilation of a satellite derived SST climatology in the heat flux formulation, with improved spatial resolution when compared to the climatology based on ship observations (COADS). In the COADS forced experiments, while the main branch of the Gulf Stream overshoots and follows a northward path, a

minor branch with reduced transport was observed to separate at Cape Hatteras. Although the satellite SST forcing was not sufficient to inhibit the overshooting, it did lead to an intensification of the separating branch.

Acknowledgements

We wish to thank C. Rooth, W. Johns, and M. Spall for helpful comments and discussions, and L. Smith for significantly improving the manuscript. E. Ryan provided the satellite-based SST fields. Support was provided by the the Office of Naval Research under contracts N00014-93-1-0404 (EPC) and N00014-95-1-0257 (AJM), and by NASA (NAGW-4329). AMP was supported by a fellowship from the Brazilian Research Council (CNPq). Computations were carried out on the CRAY T3E machines at the Pittsburgh Supercomputer Center and at the NAVO DoD High Performance Computing Center.

References

Arhan, M., 1987. On the large scale dynamics of the Mediterranean outflow. Deep Sea Res. 34 (7), 1187–1208.

Baringer, M.O., Price, J.F., 1997. Mixing and spreading of the Mediterranean outflow. J. Phys. Oceanogr. 27, 1654–1676.

Beckmann, A., Böning, C.W., Köberle, C., Willebrand, J., 1994. Effects of increased horizontal resolution in a simulation of the North Atlantic Ocean. J. Phys. Oceanogr. 24, 326–344.

Bleck, R., Chassignet, E., 1994. Simulating the oceanic circulation with isopycnic-coordinate models. In: Majundar, S.K. (Ed.), The Oceans: Physical–chemical Dynamics and Human Impact. pp. 17–39.

Bleck, R., Rooth, C., Hu, D., Smith, L.T., 1992. Salinity-driven thermocline transients in a wind- and thermohaline-forced isopycnic coordinate model of the North Atlantic. J. Phys. Oceanogr. 22 (12), 1486–1505.

Broecker, W.S., 1991. The great ocean conveyor. Oceanography 4 (2), 79–89.

Brügge, B., 1995. Near-surface mean circulation and kinetic energy in the central North Atlantic from drifter data. J. Geophys. Res. 100 (C10), 20543–20554.

Bryan, F.O., Holland, W.R., 1989. A high resolution simulation of the wind- and thermohaline driven circulation in the North Atlantic Ocean. In: Muller, P., Henderson, D. (Eds.), Parameterization of small-scale processes. Proc. 'Aha Huliko'a, Hawaiian Winter Workshop. pp. 99–115.

Bryan, K., 1984. Accelerating the convergence to equilibrium of ocean-climate models. J. Phys. Oceanogr. 14 (4), 666–673.

Bryden, H.L., Kinder, T.H., 1991. Steady two-layer exchange through the Straits of Gibraltar. Deep Sea Res. 38, 445–463.

Chassignet, E., Bleck, R., Rooth, C.H., 1995. The influence of layer outcropping on the separation of boundary currents. Part II: The wind- and buoyancy-driven experiments. J. Phys. Oceanogr. 25 (10), 2404–2422.

Chassignet, E.P., Smith, L.T., Bleck, R., Bryan, F.O., 1996. A model comparison: Numerical simulations of the North Atlantic oceanic circulation in depth and isopycnic coordinates. J. Phys. Oceanogr. 26 (9), 1849–1867.

da Silva, A.M., Young, C.C., Levitus, S., 1994. Atlas of surface marine data 1994. vol. 1: Algorithms and procedures. NOAA Atlas NESDIS 8, U.S. Department of Commerce, NOAA, NESDIS, 83 pp.

Döscher, R., Böning, C.W., Herrmann, P., 1994. Response of circulation and heat transport in the North

Atlantic to changes in thermohaline forcing in northern latitudes: a model study. J. Phys. Oceanogr. 24 (11), 2306–2320.
DYNAMO, 1997. Dynamics of North Atlantic models: simulation and assimilation with high resolution models. Technical report, Institut für Meereskunde. 334 pp.
Ezer, T., Mellor, G.L., 1992. A numerical study of the variability and the separation of the Gulf Stream, induced by surface atmospheric forcing and lateral boundary conditions. J. Phys. Oceanogr. 22, 660–682.
Hall, M.M., Bryden, H.L., 1982. Direct estimates and mechanisms of ocean heat transport. Deep Sea Res. 29, 339–359.
Holland, W.R., Bryan, F.O., 1994. Sensitivity studies on the role of the ocean in climate change. In: Malanotte-Rizzoli, P., Robinson, A. (Eds.), Ocean Processes in Climate Dynamics: Global and Mediterranean Examples. pp. 111–134.
Jia, Y., 2000. On the formation of an Azores Current due to Mediterranean overflow in a modelling study of the North Atlantic. J. Phys. Oceanogr, in press.
Joyce, T.M., Deser, C., Spall, M.A., 2000. On the relation between decadal variability of subtropical mode water and the North Atlantic Oscillation. J. Phys. Oceanogr, submitted.
Klein, B., Siedler, G., 1989. On the origin of the Azores Current. J. Geophys. Res. 94 (C5), 6159–6168.
Klinck, J.M., 1995. Thermohaline structure of an edy-resolving North Atlantic model: the influence of boundary conditions. J. Phys. Oceanogr. 25 (6), 1174–1195.
Large, W., Danabasoglu, G., Doney, S.C., McWilliams, J.C., 1997. Sensitivity to surface forcing and boundary layer mixing in a global ocean model: annual mean climatology. J. Phys. Oceanogr. 27 (11), 2418–2447.
Levitus, S., 1982. Climatological atlas of the world ocean. NOAA Prof. Paper No 13, U.S. Govt. Printing Office, 173 pp.
Macdonald, A.M., Wunsch, C., 1996. An estimate of global ocean circulation and heat fluxes. Nature 382, 436–439.
McWilliams, J.C., 1998. Oceanic general circulation models. In: Chassignet, E.P., Verron, J. (Eds.), Ocean Modeling and Parameterization. Kluwer Academic Publishers, pp. 1–44.
Nof, D., 1983. On the response of ocean currents to surface cooling. Tellus 35, 60–72.
Nurser, A.J.G., Williams, R.G., 1990. Cooling Parson's model of the separated Gulf Stream. J. Phys. Oceanogr. 20 (12), 1974–1979.
Nurser, J.G., Marsh, R., 1998. Water mass transformation theory and the meridional overturning streamfunction. Int. WOCE Newslett. 31, 36–38.
Ochoa, J., Bray, N.A., 1991. Water mass exchange in the Gulf of Cádiz. Deep Sea Res. 38 (Suppl. 1), S465–S503.
Özgökmen, T.M., Chassignet, E.P., Rooth, C.G.H., 2000. On the connection between the Medterranean outflow and the Azores Current. J. Phys. Oceanogr., accepted.
Richardson, P., 1977. On the crossover between the Gulf Stream and the western boundary undercurrent. Deep Sea Res. 24, 139–159.
Richardson, P.L., Hufford, G.E., Limeburner, R., Brown, W.S., 1994. North Brazil Current retroflection eddies. J. Geophys. Res. 99, 5081–5093.
Rios, A.F., Perez, F.F., Fraga, F., 1992. Water masses in the upper and middle North Atlantic east of the Azores. Deep Sea Res. 39 (3/4), 645–658.
Roemmich, D., Wunsch, C., 1985. Two transatlantic sections: Meridional circulation and heat flux in the Subtropical North Atlantic. Deep Sea Res. 32, 619–664.
Schmitz, W.J., 1996. On the world ocean circulation, Technical Report WHOI-96-3, Woods Hole Oceanographic Institution.
Schmitz, W.J., McCartney, M.S., 1993. On the North Atlantic circulation. Rev. Geophys. 31 (1), 29–49.
Smagorinsky, J.S., 1963. General circulation experiments with the primitive equations. I: The basic experiment. Mon. Wea. Rev. 91, 99–164.
Smith, L.T., Chassignet, E.P., Bleck, R., 2000. The impact of lateral boundary conditions and horizontal resolution on North Atlantic water mass transformations and pathways in an isopycnic coordinate ocean model. J. Phys. Oceanogr. 30, 137–159.
Spall, M.A., 1990. Circulation in the Canary Basin: a model/data analysis. J. Geophys. Res. 95, 9611–9628.
Stramma, L., 1984. Geostrophic transport in the warm water sphere of the eastern subtropical North Atlantic. J. Mar. Res. 42, 537–558.

Sun, S., 1998. Compressibility effects in the Miami Isopycnic Coordinate Ocean Model, Ph.D. thesis, University of Miami.

Townsend, T.L., Hurlburt, H.E., Hogan, P.J., 2000. Modeled Sverdrup flow in the North Atlantic from eleven different wind stress climatologies. Dyn. Atmos. Oceans 32, 373–417.

Tsuchiya, M., 1989. Circulation of the Antarctic Intermediate Water in the North Atlantic Ocean. J. Mar. Res. 47, 747–755.